

# Mobility of localized beams in non-homogeneous photonic lattices

M A Sabogal, I C Parra, M Bandera, J Gallardo and Cristian Mejía-Cortés

Programa de Física, Facultad de Ciencias Básicas, Universidad del Atlántico, Puerto Colombia 081007, Colombia.

E-mail: ccmejia@googlemail.com

**Abstract.** Waveguide arrays offer enormous potential to design circuit elements essential to fabricate optical devices capable to processing information codified by light. In this work we study the existence and stability of localized beams in one dimensional photonic lattices composed by a Kerr type waveguide array. We analyzed the case where discrete translation symmetry is broken in as much as one of the waveguides lacks a nonlinear response. Specifically, we determined the space of parameters where a coherent and robust mobility across the lattice is achieved. Moreover, we calculate the reflection and transmission coefficients when localized beams interact directly with the impurity, finding that it behaves as a variable filter depending of system parameters. Our results would shed light on develop solutions to keep unaltered information during its transmission within future optical devices.

## 1. Introduction

Localized modes have been studied extensively since middle of last century [1]. Many physical systems exhibit different phenomena which lead to formation of this kind of excitation. For example, the first system where light localization was predicted and observed was in optical fibers [2]. Here, light pulses were able to travel long distances without distortion, due to a balance between nonlinear response of material and chromatic dispersion of light [3]. This kind of pulse received the name of *optical soliton* and since then they have been widely used in telecommunications [4].

Optical periodic systems have attracted enormous attention during last three decades because they bear enormous potential in technological applications. Their underlying characteristics offer the possibility of manage the light behaviour either over long distances or short ones. For example, at big scale photonic crystal fibers, optical fibers with a micro structured cross sections [5, 6], can be employed in fiber-optics communications [7], but also they can be used as sensors with high resolution [8]. They also offer the possibility to manage light propagation in short scale. Logical operations similar to those involved with electron currents can be mimic in a completely optical “microprocessor” or photonic chip. It can be plausible due to the refractive index in theses systems possesses a periodical distribution, hence, there are forbidden regions for light propagation [9]. Experimentally, photonic lattices has been implemented by creating waveguide arrays in several media. For example, by using a femto-second pulsed laser on an amorphous (non-crystalline) phase silicon glass, it can be possible to “write” waveguides by modifying the nominal refractive index around the area where it is has been focused [10]. Photo-refractive crystals are systems where these waveguide arrays also can be written by and induction process, due to its refractive index changes by the light intensity variation, i.e., by a non-linear response of the electric field [11]. On the other hand, research on coherent transfer of light stays as a hot topic

over the years due to its direct implications in design technological devices for controlled transport of information.

A change in the periodic distribution of the refractive index, by introducing an impurity into the lattice, results in the scattering of transverse traveling waves. For example, when the impurity comes from localized solutions, the scattering of plane waves by them has opened the possibility to observe Fano resonances [12]. In a nonlinear optical context, it has been observed that scattering of solitons in waveguide arrays moving towards impurity potentials, has a complex phenomenology [13]. Moreover, by adjusting the strength of linear impurities a completely trapping regime can be tailored [14]. In the present study we address the case of nonlinear photonic lattices with an embedded linear impurity, which eventually improves the manipulation of light beam across the lattice. We hope that our results may be interesting in the design of optical limiters, barriers and gates for future photonic chips.

The paper is organized as follows: in Section 2, we introduce the model and develop the main formalism employed to identify nonlinear stationary solutions, as well as, a favorable domain in terms of system parameters to achieve coherent and robust mobility. In Section 3, we report findings on the existence and stability of localized stationary solutions around the lattice impurity. Section 4 is devoted to estimate the optimal domain for coherent and robust mobility of nonlinear modes. The analysis on scattering problem between nonlinear modes and lattice impurity is presented in Section 5. Finally, in Section 6, we summarize and draw our main conclusions.

## 2. Model

The Discrete Nonlinear Schrödinger Equation (DNLSE) represents one of the most important models in nonlinear physics. For example, in classical mechanics, this equation describes a particular model for a system of coupled anharmonic oscillators [15]. On the other hand, this model predict the existence of localized modes of excitation of Bose–Einstein condensates in periodic potentials such as those generated by counter-propagating laser beams in an optical lattice [16]. In nonlinear optics, this equation combines phenomena related to the dispersion and/or diffraction of electromagnetic waves with those generated by higher order electric polarization in periodical media [17].

When impurities are introduce to the system the translational symmetry becomes broken, which leads to the formation of localized modes around the defects [18]. For the case when the effect of impurity is the lack of nonlinear response in a specific waveguide, we can model the propagation, along the  $\hat{z}$ -axis, of the corresponding electric field amplitude present in the  $n$ -th guide,  $E_n(z)$ , as a variant of a more general DNLSE

$$i \frac{dE_n}{dz} + \zeta_{n+1} E_{n+1} + \zeta_{n-1} E_{n-1} + \gamma(1 - \delta_{n,n_i}) |E_n|^2 E_n = 0, \quad (1)$$

where  $i = \sqrt{-1}$  and  $\delta_{n,n_i}$  is the Kronecker symbol. The nonlinear response of the media is represented by the parameter  $\gamma$ , which is proportional to the nonlinear refraction index of the medium. Here we assume that  $\zeta_n$ , the coupling between waveguides, is the same for each  $n$ , i. e.,  $\zeta_n = \zeta$ . The Equation (1) has two conserved quantities, the generating function that corresponds to the Hamiltonian ( $H$ )

$$H = - \sum_{n=1}^N \left( \zeta E_n(z) E_{n+1}^*(z) + \text{c.c.} + \frac{\gamma}{2} (1 - \delta_{n,n_i}) |E_n(z)|^4 \right), \quad (2)$$

where the symbol \* and c.c. denote the complex conjugate, and the norm or optical power ( $P$ ) in the system

$$P = \sum_{n=1}^N |E_n(z)|^2. \quad (3)$$

It is worth to mention here that these two conserved quantities will be monitored during all the calculations along this work, because they will serve to check the validity of our numerical findings.

### 3. Families of nonlinear modes

We look for stationary solutions of Equation (1) in the form  $E_n = \phi_n \exp(i\lambda z)$ , where the amplitudes  $\phi_n$  are real quantities that satisfy the following system of nonlinear algebraic equations

$$-\lambda\phi_n + \zeta(\phi_{n+1} + \phi_{n-1}) + \gamma(1 - \delta_{n,n_i})\phi_n^3 = 0, \quad (4)$$

being  $\lambda$  the propagation constant of the stationary solutions. According on the sign of  $\gamma$  the nonlinear effect of the system can be of the self-focusing type ( $\gamma > 0$ ) or self-defocusing type ( $\gamma < 0$ ). Throughout the rest of the paper, we assume to deal with self-focusing type media.

We solve the model (4) by implementing a Newton-Raphson scheme. We start from a localized seed around the impurity and in a few number of iterations the algorithm converges to localized stationary solutions. We check the stability of localized solutions by performing the standard linear stability analysis. From now on we use solid (dashed) lines to denote families with stable (unstable) solutions. It is interesting to study the consequences that the value of the nonlinear constant of the impurity of the lattice entails, specifically, the type of solutions that exist around the defect and its mobility around it. Recently, it has been found that modes centered at site are the only stable family of solutions that exist around the impurity [19], however, we found that the stability region of these modes depends on the value of the nonlinearity of impurity.

Figure 1(a) shows the families of solution in the space of  $(P, \lambda)$  for the even and odd modes far from the defect. Families for odd modes around the defect for ten values of  $\gamma_i$  between 0 and 0.90 is displayed at Figure 1(b). It can be seen here that when nonlinearity for defect diminish there is a reduction in the region of existence and stability of this solutions. The inset in Figure 1(a) sketches the odd (c) and even (d) modes belonging to the families represented by solid and dashed curves, respectively. On the other hand, bottom inset at Figure 1(b) displays three modes around the impurity that belongs to the odd (e), even (f) and symmetrical (g) families of solution, when  $\gamma = 0$ , for three different values of  $\lambda$ . Last two families are not illustrated in this work but they have been reported recently in reference [19].

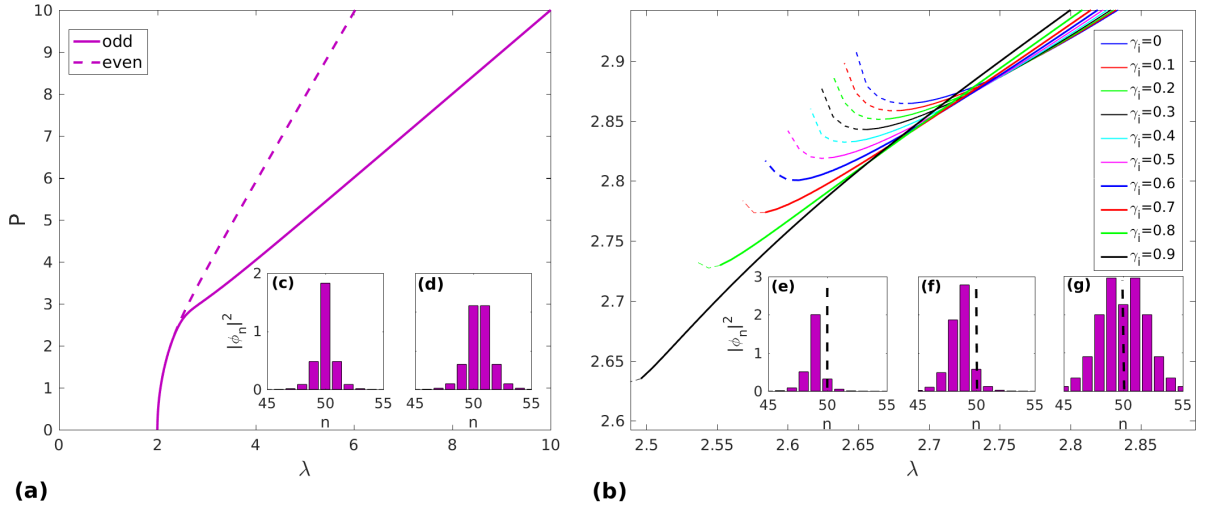


**Figure 1.** (a)  $P$  vs  $\lambda$  diagram for odd and even families of solutions far away from the impurity. Bottom inset displays both solutions for  $P = 3.00$  and  $\lambda = 2.85$  (c) and  $2.62$  (d), respectively. (b)  $P$  vs  $\lambda$  diagram for odd families around impurity for different values of  $\gamma$ . Bottom inset displays three different type solutions, near to impurity for  $P = 3.00$ ,  $\gamma = 0$  and  $\lambda = 2.91$  for the odd mode (e),  $\lambda = 2.66$  for even mode (f) and  $\lambda = 2.28$  for symmetrical mode (g).

#### 4. Mobility of localized modes

With the aim to study the interaction between solitons and the linear impurity, it is mandatory to determine the zones in the space  $(P, k)$  of powers and momentum, in which coherent mobility is guaranteed. It is well known that the mobility of discrete solitons is restricted by the Peierls-Nabarro (PN) barrier [18], which exists due to the non-integrability of the DNLSE [20, 21]. This barrier can be estimated as the difference in energy ( $H$ ) between the solutions of the fundamental modes, sketched at top left inset in Figure 1(a). By applying a power constraint to the Newton-Raphson method we could compare the value of the Hamiltonian (energy) of the modes that have the same power [22]. In that way, we can identify those regions where  $H$  is similar, both for odd and even modes, which implies that these solutions, previously endowed with momentum, can move across the lattice in an adiabatic way, i. e., they can transform dynamically into the another one almost without radiating energy and preserving their shape. It is well known that for the Kerr nonlinearity, there is a critical power where PN barrier is large enough for the soliton to be confined in the initial guide [23]. In order to determine these zones, solitons with different configurations of  $k$  and  $P$  were propagated. For the case of good mobility, their effective displacement was quantified, in terms of their center of mass  $CM := \sum_{n=1}^N n|\phi_n|^2/P$ , as shown in Figure 2(a).

It is clear that for power greater than  $P \approx 3.00$  the mobility of the soliton is almost zero no matter which was the impinged momentum on the mode. In order to select optimal parameter domain where coherent mobility is guaranteed we calculate the maximum variation of the velocity angle of the center of mass, along the propagation distance with respect to the initial angle. In Figure 2(b) it can be observed that for values greater than  $P \approx 2.50$  the variation of the initial angle is greater than 5.00 degrees and independent of the momentum. We also refine our procedure by identifying the maximum distance at which the initial angle is conserved, undergoing a change of less than 10.00% for different configurations of  $k$  and  $P$ . As shown in Figure 2(c), for powers below  $P \approx 2.30$  the criterion is fulfilled for the entire propagation distance. The above suggests that the range  $|k| \leq \pi/9$  and  $P < 2.30$  ensures a coherence mobility of the information.

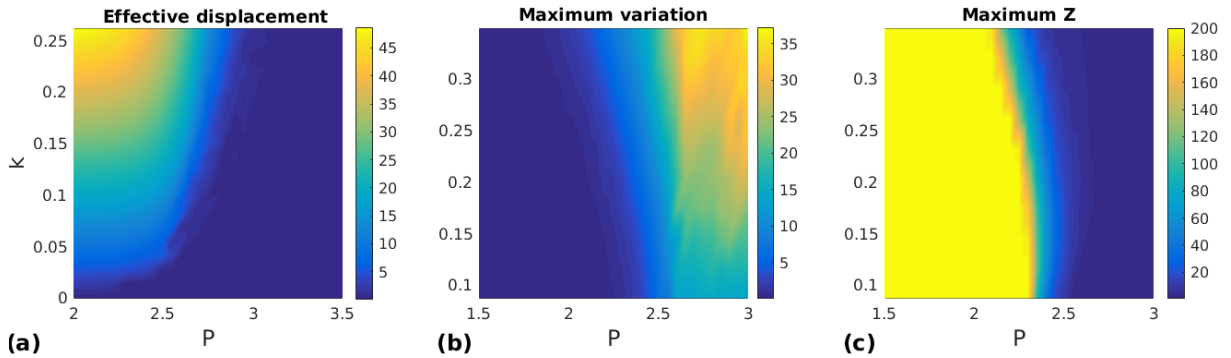


**Figure 2.** Effective displacement of the center of mass (a), maximum variation of the velocity angle of the center of mass (b) and maximum distance at which change in the velocity angle is below 10.00% (c), as function of  $P$  and  $k$ .

#### 5. Pulse transmission

Let us now consider the interaction between a discrete soliton, endowed with a transverse momentum  $k$ , and one impurity located at  $n_i = N/2$ . We numerically integrate the model (1) with a Runge Kutta scheme by taking as initial condition  $\phi_n^k = \phi_n \exp(ikn)$ , being  $\phi_n$  a stationary mode of the system. When the soliton reaches the impurity, the radiation can be reflected, transmitted and/or captured. To analyze the soliton-impurity interaction we define the reflectance ( $R$ ), transmittance ( $T$ ) and the capture

fraction ( $C$ ) coefficients as

$$R := \frac{\sum_{n=1}^{n_i-\Delta} |\phi_n|^2}{\sum_{n=1}^N |\phi_n|^2}, \quad T := \frac{\sum_{n=n_i+\Delta}^N |\phi_n|^2}{\sum_{n=1}^N |\phi_n|^2}, \quad C := \frac{\sum_{n=n_i-\Delta}^{n_i+\Delta} |\phi_n|^2}{\sum_{n=1}^N |\phi_n|^2}. \quad (5)$$

Here  $\Delta$  is defined as the size of the impurity. As we are dealing with conservative systems, it is clear that the condition  $R + T + C = 1$  must be fulfilled during beam evolution. It has been observed that when solitons of the same power with different  $k$  are sent toward the impurity, there is a critical momentum  $k_c$  for which the soliton is trapped around the defect [19]. Therefore, for values  $k < k_c$  the solitons are reflected and for  $k > k_c$  they are transmitted. We observe a similar behavior here, by varying the optical power of the soliton with a fixed  $k$ , which interacts with the impurity. As can be seen from Figure 3(a), it is clear that impurity behaves like a filter once the power of modes is near to  $P_c \approx 1.674$ , namely, the critical power. Around this value of  $P_c$  there exist a narrow region where light can be trapped by the impurity [cf. Figure 3(b)] over significant distances of propagation. Below this critical power ( $P_c$ ), the radiation becomes transmitted almost entirely as is illustrated in Figure 3(c).

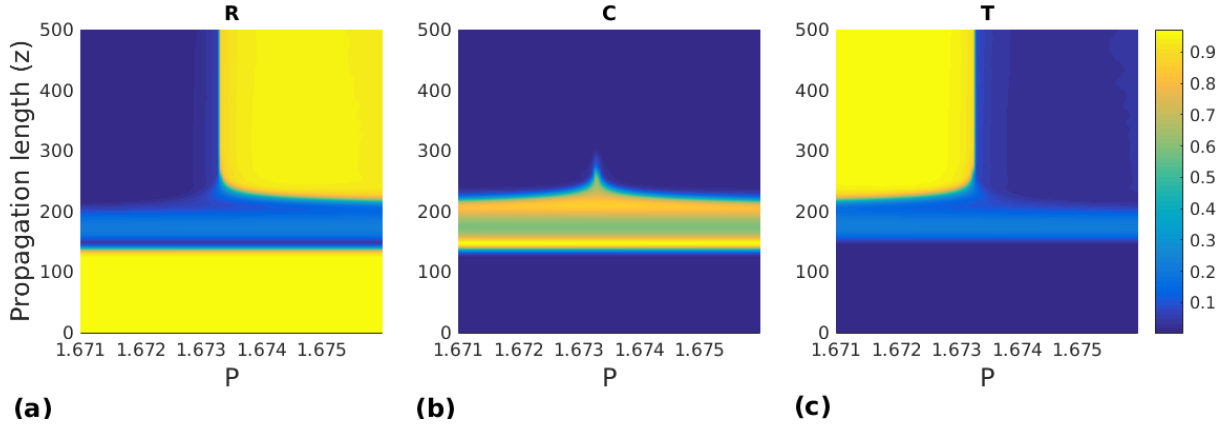


**Figure 3.** Reflection (a), Capture (b) and Transmission (c) coefficients as function of  $P$  and  $z$  near of the critical power  $P_c = 1.6732$ , for  $k = \pi/18$ ,  $\zeta = \gamma = 1.00$  and  $\gamma_i = 0$ .

With the aim to have a more detailed landscape on how the optical power and the transverse momentum affect the soliton-impurity interaction, we analyze the propagation of solitons with different configurations of  $k$  and  $P$ , moving towards the defect, for two different values of  $\gamma_i$ . In order to ensure a consistent estimation of  $R$ ,  $C$  and  $T$  coefficients, we are going to calculate coefficients at the longitudinal distance  $z$ , after the collision with the impurity, equal to the longitudinal distance that they had to travel before to collide with. Figure (4) display these coefficients for two values of nonlinear parameter; upper row for  $\gamma_i = 0.90$  and lower row for  $\gamma_i = 0.00$ . Domains where total reflection  $R$  and transmission  $T$  are guaranteed in each case are displayed in first and third column, respectively. Likewise, sub-spaces where solitons can be trapped around the impurity correspond with bright spots in middle column. Finally, comparing the two cases, it is observed that by increasing the value of the nonlinearity of the defect, a shift or increase in the critical values for which the impurity behaves like a filter is obtained, approaching the homogeneous regime when the order between the nonlinear constant of the impurity and the network tends to one.

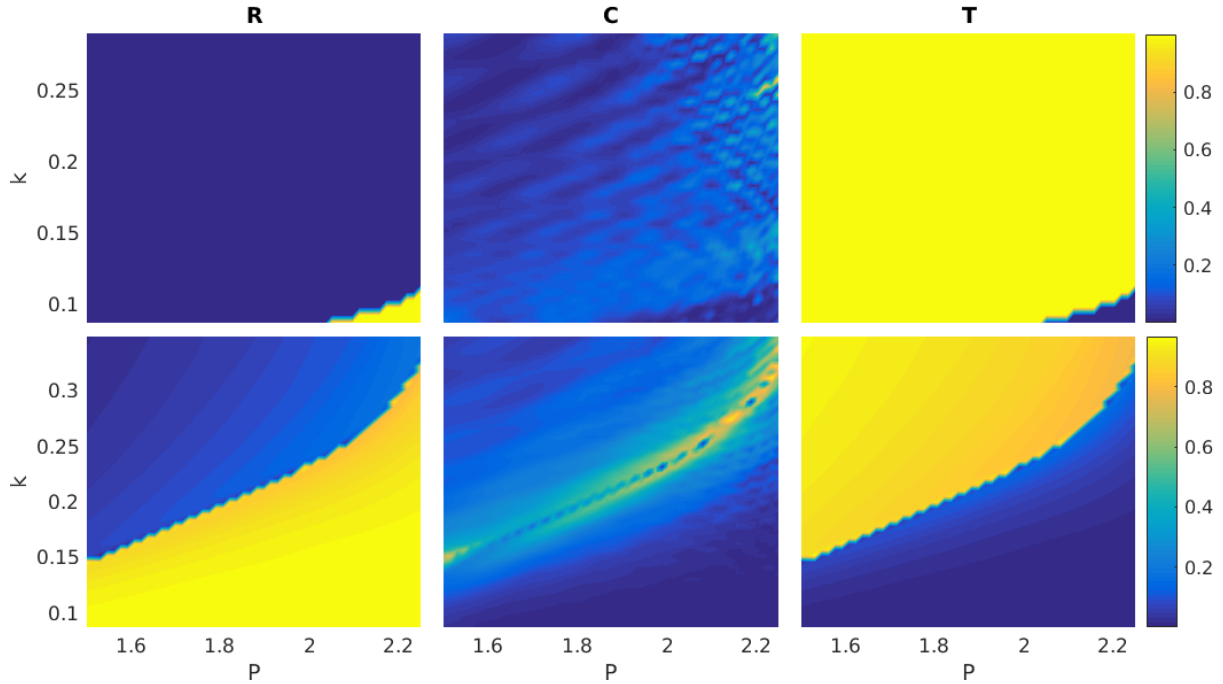


**Figure 4.** Color map of the coefficients (R) Reflectance (C) Capture and (T) Transmittance as function of the transverse momentum  $k$  and the optical power, for  $\zeta = \gamma = 1.00$  and  $\gamma_i = 0.90$  for the upper row and  $\gamma_i = 0.00$  for the lower row.

## 6. Conclusions

In this work we address the problem of interaction between discrete solitons and a linear impurity in a photonic lattice composed by a one dimensional waveguides array. To do that, we begun calculating the stationary modes that exist around the defect. The analysis of the mobility of solitons far away from impurity allow us to determine the areas where the high mobility and coherence of information is guaranteed, as function of the transverse momentum and the optical power. The interaction between the impurity and the nonlinear modes displays a corpuscular dynamic. The regions of reflectance and total transmittance in which the impurity behaves as an optical limiter were determined. Besides, domains for critical power and momentum values in which the soliton is trapped around the impurity where identified. Depending of the subspace in the parameter space we observe drastic change in the reflectance and transmittance coefficients as function of  $\gamma_i$ . We hope that these results may be interesting in the design of optical limiters for solitons, that allow optimization of the manipulation and transmission of information within novel photonic chips. We pretend to extend this kind of analysis in systems with more dimensions, as well as, those ones with exotic dispersion relations.

## References

- [1] Anderson P W 1958 *Phys. Rev.* **109**(5) 1492–1505
- [2] Hasegawa A and Tappert F 1973 *Applied Physics Letters* **23** 142–144
- [3] Arévalo E, Ramírez C and Guzmán A 1995 *MOMENTO* **0**
- [4] Segovia F A and Cabrera E 2015 *Redes de Ingeniería* **6** 26–32
- [5] Russell P S 2006 *J. Lightwave Technol.* **24** 4729–4749
- [6] Russell P 2003 *Science* **299** 358–362
- [7] Roberts P J, Couny F, Sabert H, Mangan B J, Williams D P, Farr L, Mason M W, Tomlinson A, Birks T A, Knight J C and Russell P S 2005 *Opt. Express* **13** 236–244
- [8] Cregan R F, Mangan B J, Knight J C, Birks T A, Russell P S J, Roberts P J and Allan D C 1999 *Science* **285** 1537–1539
- [9] Joannopoulos J D, Villeneuve P R and Fan S 1997 *Nature* **386** 143–149
- [10] Szameit A and Nolte S 2010 *Journal of Physics B: Atomic, Molecular and Optical Physics* **43** 163001

- [11] Armijo J, Allio R and Mejía-Cortés C 2014 *Opt. Express* **22** 20574–20587
- [12] Fano U 1961 *Phys. Rev.* **124**(6) 1866–1878
- [13] Linzon Y, Morandotti R, Volatier M, Aimez V, Ares R and Bar-Ad S 2007 *Phys. Rev. Lett.* **99**(13) 133901
- [14] Morales-Molina L and Vicencio R A 2006 *Opt. Lett.* **31** 966–968
- [15] Eilbeck J C and Johansson M 2003 The discrete nonlinear schrödinger *Proc. 3rd Conf.: Localization and Energy Transfer in Nonlinear Systems* p 44
- [16] Franzosi R, Livi R, Oppo G L and Politi A 2011 *Nonlinearity* **24** R89–R122
- [17] Khare A, Rasmussen K Ø, Salerno M, Samuelsen M R and Saxena A 2006 *Physical Review E* **74** 016607
- [18] Kevrekidis P G 2009 *The discrete nonlinear Schrödinger equation: mathematical analysis, numerical computations and physical perspectives* vol 232 (Springer Science & Business Media)
- [19] Mejía-Cortés C, Cardona J, Sukhorukov A A and Molina M I 2019 *Physical Review E* **100** 042214
- [20] Brazhnyi V A, Jisha C P and Rodrigues A 2013 *Physical Review A* **87** 013609
- [21] Peschel U, Morandotti R, Arnold J M, Aitchison J S, Eisenberg H S, Silberberg Y, Pertsch T and Lederer F 2002 *JOSA B* **19** 2637–2644
- [22] Lederer F, Stegeman G I, Christodoulides D N, Assanto G, Segev M and Silberberg Y 2008 *Physics Reports* **463** 1–126
- [23] Ahufinger V, Sanpera A, Pedri P, Santos L and Lewenstein M 2004 *Physical Review A* **69** 053604